



Short communication

## Biopatterning for label-free detection

Julie M. Goddard<sup>a,1</sup>, Sudeep Mandal<sup>b</sup>, Sam R. Nugen<sup>c</sup>, Antje J. Baeumner<sup>c</sup>, David Erickson<sup>a,\*</sup>

<sup>a</sup> Sibley School of Mechanical and Aerospace Engineering, Cornell University, Ithaca, NY 14853, USA

<sup>b</sup> Applied and Engineering Physics, Cornell University, Ithaca, NY 14853, USA

<sup>c</sup> Biological and Environmental Engineering, Cornell University, Ithaca, NY 14853, USA

### ARTICLE INFO

#### Article history:

Received 14 November 2008

Received in revised form 29 July 2009

Accepted 27 October 2009

Available online 1 November 2009

#### Keywords:

Biopatterning

Biosensors

Label-free detection

Microfluidics

Surface chemistry

### ABSTRACT

We present a biopatterning technique suitable for applications which demand a high degree of surface cleanliness, such as immobilization of biological recognition elements onto label-free biosensors. In the case of label-free biosensing, the mechanism of signal transduction is based on surface bound matter, making them highly sensitive to surface contamination including residues left during the biopatterning process. In this communication we introduce a simple, rapid processing step that removes 98% of the residues that often remain after standard parylene lift-off patterning. Residue-free parylene biopatterning is combined with microfluidics to localize biomolecule immobilization onto the sensing region and to enable multiplexed biopatterning. We demonstrate the applicability of this method to multiplexed label-free detection platforms by patterning nucleic acid capture probes corresponding to the four different serotypes of Dengue virus onto parallel 1D photonic crystal resonator sensors. Scanning electron microscopy (SEM) and atomic force microscopy (AFM) are used to quantify surface cleanliness and uniformity. In addition to label-free biosensors, this technique is well suited to other nanobiotechnology patterning applications which demand a pristine, residue-free surface, such as immobilization of enzymes, antibodies, growth factors, or cell cultures.

© 2009 Elsevier B.V. All rights reserved.

### 1. Introduction

Label-free biosensors are a promising class of biomolecular detectors because they bypass the need for a fluorescent, radio, or enzymatic label. Dependence on such a label to detect a biomolecular interaction often adversely impacts device performance, either by interfering with the binding event (false negative) or by non-specific adsorption of the labeling molecule (false positive) [1]. There are a number of emerging techniques that permit direct label-free detection of bound target biomolecules [2], including optical [3–5], electrical [6], and acoustic sensors [7]. While the method of signal transduction varies between the different label-free techniques (*i.e.* a change in local refractive index for optical biosensors, resonant frequency for mechanical biosensors, or current/impedance for electrical biosensors), the principle of detection is uniform in that they all respond to surface bound matter. Label-free techniques are therefore highly sensitive to surface con-

tamination. Fig. 1 illustrates several mechanisms by which surface contamination can hinder the performance of label-free biosensors.

While there are a number of published reports on the design and fabrication of ultrasensitive nanobiosensors, there remain challenges in patterning biomolecular recognition elements in ways that both confine the immobilization to the sensing element and result in a pristine, residue-free surface. Microarray and inkjet printing are widely used biopatterning techniques, but their resolution is limited to a spot size between 10  $\mu\text{m}$  and 100  $\mu\text{m}$ . Additionally, the potential for capillary flow along micro- and nanofabricated topography makes these techniques less suitable for confinement of immobilized biomolecules. Microcontact printing offers biopatterning on the scale of several micrometers, but the stamp can foul the surface, affecting device sensitivity as described above [8–10]. Parylene biopatterning has proven to be an effective means to immobilize biomolecules onto surfaces on the micrometer scale or smaller [11–14]. Unfortunately, it has been observed that a “grassy” parylene residue often remains on the substrate after lithographic processing. This residue may be a result of contaminants from within the coating chamber incorporating within the parylene thin film during deposition. Metal contaminants embedded within the parylene thin film can form stable complexes with oxidized parylene [15], which are then resistant to complete etching. The origin of the residues notwithstanding, we have observed that extending the etch time does not reduce

\* Corresponding author at: Sibley School of Mechanical and Aerospace Engineering, Cornell University, 240 Upson Hall, Ithaca, NY 14853, USA. Tel.: +1 607 255 4861; fax: +1 607 255 1222.

E-mail address: [de54@cornell.edu](mailto:de54@cornell.edu) (D. Erickson).

<sup>1</sup> Current address: Department of Food Science, University of Massachusetts, Amherst, Massachusetts, 01003, USA.

or remove the residues. Because parylene is biocompatible and has low intrinsic fluorescence, such residue may not affect performance of biosensors that use a fluorescent or enzymatic label in their signal transduction. However, in the development of label-free biosensors, surface contamination reduces signal intensity which adversely impacts device sensitivity [16].

It has been suggested that photooxidation of parylene may result in low molecular weight oxidation products [15]. Indeed, long-term UV irradiation has been reported to affect the optical, thermal, and electrical properties of parylene thin films [17]. UV irradiation of polymer surfaces generates carbon radicals, which are then subject to attack by atmospheric oxygen. Pruden et al. [18] characterized photooxidation products of Parylene-C following various levels of UV exposure at 254 nm. Using Rutherford backscattering in combination with secondary ion mass spectrometry, they concluded that UV oxidized Parylene-C contains a range of oxygenated moieties, including carboxylic acids, with the majority of these oxidation products occurring in the top 300–500 nm of the UV exposed surface.

It was our hypothesis that parylene residues that remain after lithographic patterning could be oxidized by UV irradiation to base-soluble low molecular weight oligomers. In this communication we present a rapid, facile technique to eliminate surface residues that often remain after parylene biopatterning, making it suitable for patterning onto label-free biosensor transduction elements. The technique is developed using clean, unstructured silicon wafers. We then demonstrate this technique by patterning nucleic acid capture probes onto parallel 1D photonic crystal resonators fabricated via E-beam lithography out of silicon-on-insulator (SOI). The design, fabrication, characterization, and biosensor function of these photonic biosensors are the subject of other papers [5,19].

## 2. Materials and methods

### 2.1. Materials

MicroPrime P-20 was purchased from MicroPrime™ (Phoenix, AZ, USA). Microposit S1818® positive photoresist was purchased from Rohm and Haas (Marlborough, MA, USA). AZ300-MIF photoresist developer was purchased from AZ Electronic Materials (Somerville, NJ, USA). Aminopropyltrimethoxysilane (APTMS) was purchased from TCI America (Portland, OR, USA). Generation 4.5 polyamidoamine (G(4.5) PAMAM) carboxyl terminated dendrimers were purchased from Dendritech, Inc. (Midland, MI, USA). 1-Ethyl-3-(3-dimethylaminopropyl) carbodiimide (EDC) was purchased from G-Biosciences (Maryland Heights, MO, USA). *N*-Hydroxysuccinimide (NHS) was purchased from MP Biomedicals, LLC (Solon, OH, USA). Polydimethylsiloxane (PDMS, Sylgard 184) components were purchased from Dow Corning (Midland, MI, USA).

DNA probes that have been optimized to capture the four serotypes of Dengue virus [20–24] were synthesized by Operon Biotechnologies (Huntsville, AL, USA). Capture probes were 5' modified with an amine functionality and 3' modified with TAMRA-Q fluorescent dye. All probes were diluted to 300  $\mu$ M in 0.1 M phosphate buffer, pH 8.5, containing 1 mM ethylenediamine tetraacetic acid (EDTA) and 0.01 wt% sodium azide and stored at  $-20^{\circ}\text{C}$  until use. All other reagents were laboratory grade or better and were used as received.

### 2.2. Surface patterning

Clean silicon wafers were used to quantitatively characterize the presence of parylene residues after various treatment conditions using AFM. Once an optimal treatment was identified, the improved parylene biopatterning technique was demonstrated on

the photonic crystal biosensors, the design and demonstration of which are the subject of separate papers [5,19]. The chemistries and biopatterning techniques described herein perform equally well on unstructured silicon wafers and SOI photonic crystal biosensors. In order to prepare the silicon substrates for capture probe immobilization, silicon substrates were submerged in piranha solution (3:1 mixture of concentrated sulfuric acid and 30% hydrogen peroxide) for 30 min, followed by rinsing in copious Milli-Q water in order to clean the surface and generate surface silanol (Si-OH) groups. A 1  $\mu$ m film of Parylene-C was vapor deposited onto clean silicon substrates using a model PDS-2010 Labcoater 2 (Specialty Coating Systems, Indianapolis, IN). MicroPrime P-20 was spun on the substrates at 3000 rpm for 30 s to ensure proper adhesion of photoresist to parylene. Microposit® S1818 positive photoresist was then spun at 3000 rpm for 30 s to a thickness of approximately 2  $\mu$ m, followed by a 60 s prebake at  $115^{\circ}\text{C}$ . When the parylene patterning was conducted on structured SOI photonic crystals, the parylene stencil was aligned using alignment marks present on both the photonic crystal substrate and the stencil photomask. Substrates were exposed through a photomask for 4.5 s at 405 nm using an HTG System III-HR Contact Aligner, after which they were agitated for 90 s in AZ300-MIF developer, rinsed in deionized water, and finally dried under nitrogen. Following a 10 min oxygen plasma chamber clean and a 10 min platen cool down, the exposed parylene was etched for 7 min in a Plasmatherm SLR-720 reactive ion etcher (30 sccm  $\text{O}_2$ , 60 mTorr, 150 W).

Grassy parylene residue was removed by treating the etched substrates in a UV cleaner (Samco, Inc., Sunnyvale, CA) and dissolving the photooxidized residue product in an alkaline solution. Various UV/base conditions were tested, from which it was determined that one minute exposure (10 mW/cm<sup>2</sup>, 254 nm), followed by 1 min rinsing in deionized water adjusted to pH 12 by sodium hydroxide provided the desired result without impacting the bulk parylene. Following UV/base treatment, substrates were rinsed in ethanol to remove residual photoresist. Etched parylene substrates rinsed for 1 min in neutral deionized water served as control. Surface topography of parylene patterned substrates was evaluated by scanning electron microscopy (SEM) and atomic force microscopy (AFM, DI-3000, Veeco Instruments, Inc., Woodbury, NY) with and without UV/base treatment. Roughness values and effective surface areas ( $n=4$ , two samples on each of two independent chips) were calculated from atomic force micrographs using Gwyddion SPM data analysis software.

### 2.3. Surface functionalization and immobilization of nucleic acid probes

After parylene patterning and UV/base treatment, silicon substrates were surface modified and DNA capture probes were covalently linked to the patterned, functionalized substrate. Parylene patterned SOI photonic biosensors were shaken in 2% APTMS in 95% ethanol for 5 min, followed by rinsing in ethanol and water, and drying under air. APTMS-functionalized substrates were baked at  $80^{\circ}\text{C}$  for 1 h for silane curing. Generation 4.5 carboxylic acid terminated dendrimers were covalently bound to aminated substrates using water-soluble carbodiimide chemistry, to generate carboxy-functionalized surfaces. Detail about the surface chemistry used in this communication is available in Goddard and Erickson [25]. Substrates were shaken for 2 h at room temperature in a solution of 10  $\mu$ M dendrimer in 0.067 M phosphate buffer, pH 7.4, containing 14 mM EDC and 0.7 mM NHS, followed by rinsing in deionized water and drying under air. Subsequently, amine-terminated DNA capture probes were bound to the carboxyl-functionalized SOI photonic biosensor surfaces via the two-step water-soluble carbodiimide chemistry [26]. Briefly, surfaces were first shaken for 15 min in 0.1 M 2-(*N*-morpholino)ethanesulfonic acid (MES) buffer,

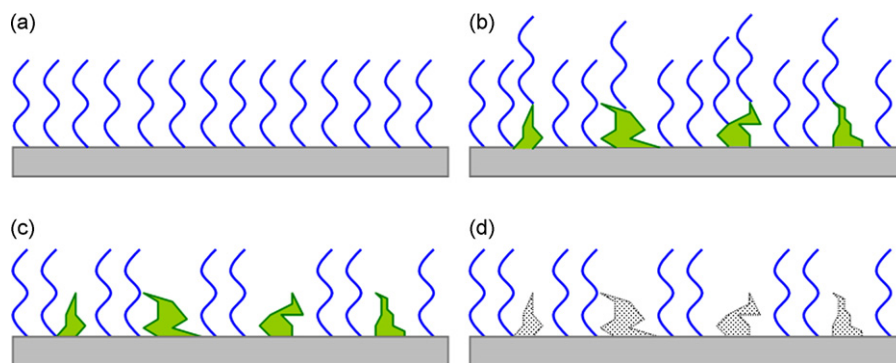


**Fig. 1.** Effect of surface contamination on sensitivity of label-free biosensing techniques. (a) Uniform immobilization of biological recognition element, no contamination present; (b) some biological recognition elements are non-covalently coated over contaminants, extending biomolecular interaction further from sensing surface, thus reducing device sensitivity; (c) contaminants reduce the number of covalently bound biological recognition elements, thus limiting the number of potential biomolecular interactions; (d) contaminants that delaminate from the sensing surface during detection assay result in a signal that suggests less bound mass than before baseline readings.

pH 6, containing 50 mM EDC and 5 mM NHS, followed by rinsing in water and drying under air. In order to separately address parallel resonators such that a different capture probe could be immobilized on each resonator, a microfluidic functionalization technique was employed (Fig. 2). Soft lithography fluids were prepared by casting a 1:10 mixture (curing agent:base) of PDMS over a positive relief master [27]. After punching inlet and outlet ports, PDMS microchannels were placed over the EDC and NHS activated dendrimer functionalized surface, and secured with a custom plexiglass housing. Amine-terminated DNA probes, which were stored in pH 8.5 buffer as described above, were diluted to 150  $\mu$ M in 0.1 M MES buffer, pH 5.0 (final conjugation buffer was pH 7.0). Probes were withdrawn through microchannels for 2 h at room temperature, followed by in-channel water rinsing. SOI photonic biosensors patterned with nucleic acid capture probes were then removed from the plexiglass housing, PDMS microchannels and parylene film were peeled off the substrate, and the substrate was rinsed in deionized water and air dried.

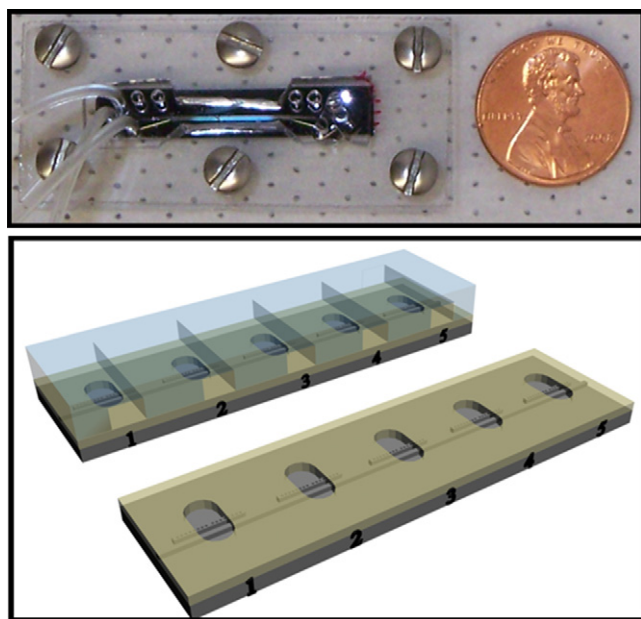


**Fig. 2.** Microfluidic functionalization of multiplexed label-free biosensors. (Top) Experimental setup: parylene patterned substrate and PDMS microfluidics are held together by custom polymethyl methacrylate housing. (Bottom) Schematic of microfluidic targeting of individual SOI photonic sensors by parylene patterning combined with PDMS microfluidics.

### 3. Results and discussion

#### 3.1. Uniformity of patterned silicon substrates

SEMs of control and UV/base treated parylene patterned substrates were taken to elucidate the effect of UV/base treatment on uniformity and cleanliness of parylene patterned substrates, as well as the ability to target separate nucleic acid capture probes over the parallel SOI photonic biosensors (Fig. 3). As described above, surface contaminants such as parylene residue can reduce the signal transduced by a given biomolecular interaction, either by extending such an interaction away from the high sensitivity region of the sensor surface (Fig. 1b) or by limiting the number of potential interactions (Fig. 1c). In addition, contaminants present during functionalization that are removed from the surface during the detection assay result in confusing signal, indicating an apparent reduction in bound biomolecule (Fig. 1d). Indeed, since nanometer-scale coatings have been reported to cause significant red-shifts in optical devices [28], device sensitivity will be affected by any residue. Exposure of etched parylene to UV irradiation for 1 min, followed by 1 min rinsing in deionized water adjusted to pH 12 by sodium hydroxide effectively removed the residual parylene (Fig. 3b). It was experimentally determined that longer etch times degraded the integrity of the bulk parylene such that it could not be removed intact. Shorter etch times and lower pH rinses were ineffective in removing all of the residues, and higher pH rinses were avoided to prevent etching of the SOI photonic nanostructures.

After UV/base treatment and immobilization of four nucleic acid probes over parallel resonators (details on probe immobilization follow), the parylene remained intact and was fully removed (Fig. 3c). Immobilized capture probes appear slightly darker due to differences in charging effects during SEM imaging between the biopatterned region and the unfunctionalized  $\text{SiO}_2$  substrate. For reasons described above, it is important to note the absence of observable parylene residues or other contaminants on the final patterned device (Fig. 3c).

Atomic force microscopy (AFM) was employed in order to better quantify the effect of the UV/base treatment on changes in surface roughness (Fig. 4). The UV/base treatment utilized here reduced the root mean square roughness from  $69.7 \pm 5.4$  nm to  $1.3 \pm 0.1$  nm. This final roughness is similar to root mean square roughness values of cleaned Si substrates, which are reported to range from 0.5 nm to 2.0 nm [29]. UV irradiation is reported to penetrate 300–500 nm into the surface of parylene [18]; it therefore follows that residues of the observed roughnesses ( $69.7 \pm 5.4$  nm) would be fully oxidized by UV irradiation, and subject to base dissolution, while the

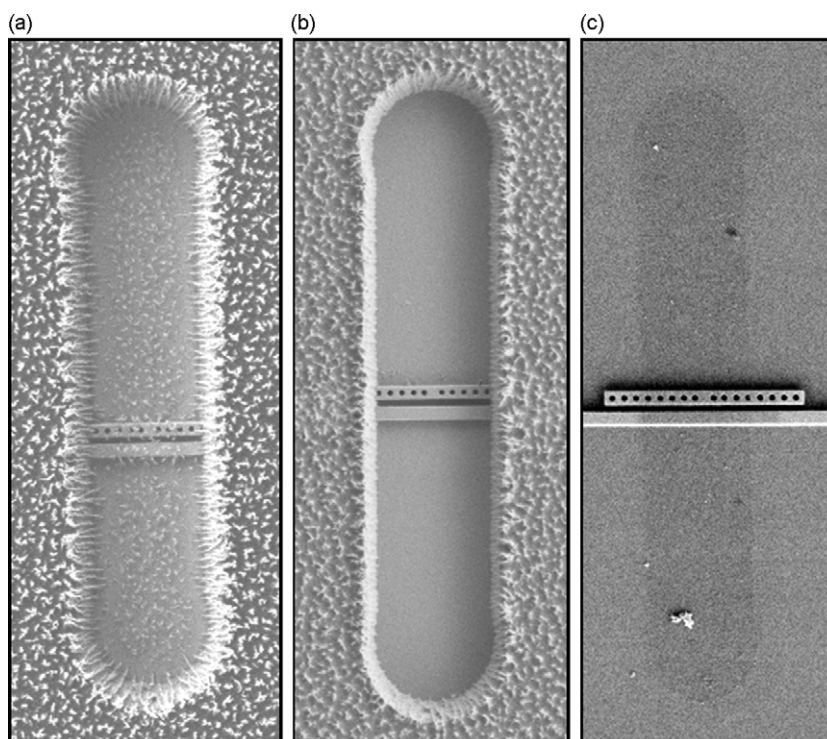


**Fig. 3.** SEM of parylene etched optical nanostructures. (a) without UV/base treatment, and (b) with UV/base treatment. (c) SEM image after removal of parylene. Darkened spot shows location of probes (see also fluorescence image in Fig. 5). The photonic crystal resonator measures 450 nm in width, 6.5  $\mu\text{m}$  in length.

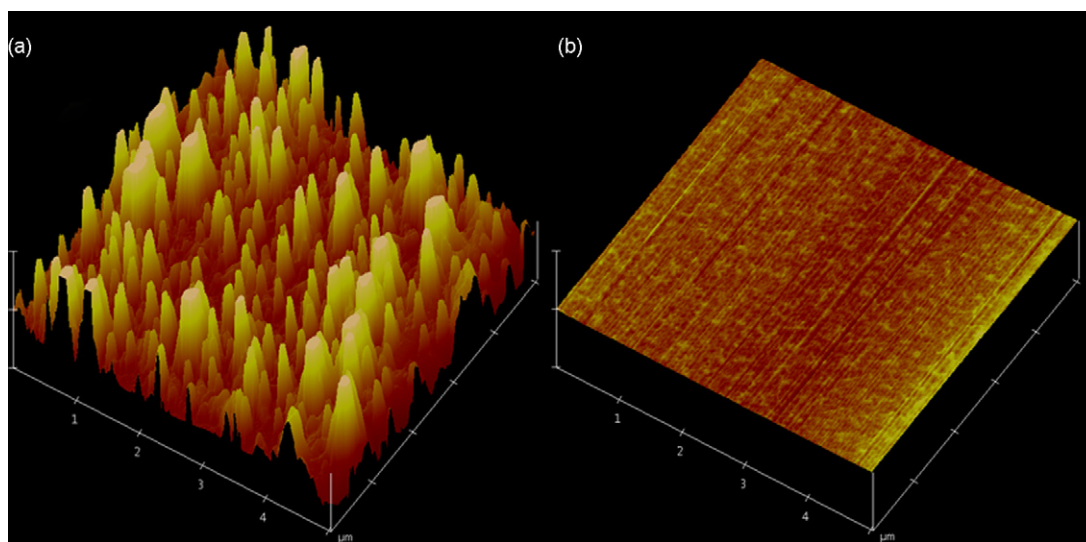


**Fig. 4.** Representative AFM images of etched parylene (a) without UV/base treatment, and (b) with UV/base treatment. Both images are 5  $\mu\text{m}$   $\times$  5  $\mu\text{m}$  in X and Y and 300 nm in Z.

bulk parylene (film thickness of 1  $\mu\text{m}$ ) would remain intact. It is interesting to note that in addition to the nearly two log reduction in surface roughness, the treatment also improved surface uniformity, as indicated by deviation of roughness values. As described above, surface contamination adversely affects label-free biosensor performance both by the height of the residues, as well as the surface coverage. Effective surface area was also calculated to quantify the effect of the UV/base treatment. Effective surface area is a calculation which accounts for the three dimensional nature of a topographical substrate, such as when residues are present. For example, a pristine two-dimensional surface measuring 5  $\mu\text{m}$   $\times$  5  $\mu\text{m}$  would have an effective surface area of 25  $\mu\text{m}^2$ .

Increasing the roughness of the surface increases the effective surface area. The UV/base treatment decreased the effective surface area from  $47.2 \pm 1.44 \mu\text{m}^2$  to  $25.1 \pm 0.02 \mu\text{m}^2$  (surface area of a pristine 5  $\mu\text{m}$   $\times$  5  $\mu\text{m}$  spot is 25  $\mu\text{m}^2$ ). The increased effective surface area not only reduces device sensitivity for the reasons illustrated in Fig. 1, but also increases the surfaces available for non-specific binding, which further reduces device sensitivity. As with the roughness measurements, effective surface area was not only significantly reduced in value, but also was made more uniform, as evidenced by the lower deviation in treated substrates. The impact of surface uniformity on device performance becomes greater as the interrogated region becomes smaller, as in our SOI

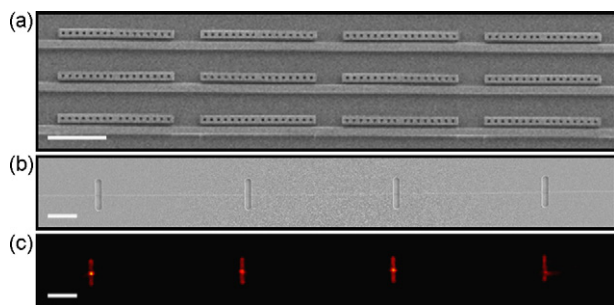


**Fig. 5.** (a) SEM of an array of parallel resonators (scale bar is 3  $\mu\text{m}$ ). (b) SEM of parallel parylene patterned 1D photonic crystal resonators (scale bar is 20  $\mu\text{m}$ ). (c) Fluorescence micrograph of patterned capture probes after parylene removal (scale bar is 20  $\mu\text{m}$ ).

photonic crystal biosensors, which each have a surface area on the order of  $\sim 5 \mu\text{m}^2$  [5,19]. While the effect of such deviations can be averaged out over a larger area, in order to have consistent measurements on the micrometer scale it is critical to minimize not only the presence of residues but also deviation of residue roughness and effective surface area, as we have done by our UV/base treatment.

### 3.2. Biopatterned substrates

After a suitable treatment for removing parylene residue was developed using silicon wafers, we demonstrated the utility of the technique on SOI photonic crystal biosensor chips. These chips have waveguides with adjacent one-dimensional photonic crystal resonators. The waveguides and resonators measure 250 nm in height and 450 nm in width; each photonic crystal possesses 16 holes (200 nm in diameter) and a central cavity of varying size which tunes the resonant wavelength [5]. After successful removal of trace parylene residues, SOI photonic biosensors were surface modified and DNA capture probes were covalently linked to the patterned, functionalized substrates. PDMS microfluidics provide a useful means to individually target separate transduction elements within a biosensor allowing for multiplexed detections. After microfluidic immobilization of multiple biorecognition elements, the functionalization fluidics can be removed, and a separate set of detection fluidics can be applied. Unfortunately, uncrosslinked oligomers from the PDMS microfluidics can leave a residue on the substrate, affecting device performance as described above. By coupling the fluidic functionalization step with parylene biopatterning, the substrate is protected from such contamination by the parylene film, which is then removed before the detection fluidics are applied, leaving a pristine surface with biopatterned regions. Fig. 5 illustrates the targeted patterning of four nucleic acid capture probes over parallel optical nanostructures. Combining the improved parylene biopatterning technique with microfluidic functionalization, we are able to immobilize different capture probes over each of four different resonators, allowing for multiplexed sensing capabilities in the future.

## 4. Conclusion

In summary, we have established a simple means to reduce the grassy parylene residue that often remains after standard parylene biopatterning processing, and immobilized nucleic acid probes by a silane and dendrimer linkage. One minute UV irradiation (254 nm, 10 mW/cm<sup>2</sup>) followed by 1 min rinsing in dilute base solution eliminated 98% of parylene residue. Removal of residue and quantification of changes in roughness and surface uniformity were confirmed by AFM and SEM. By using parylene

patterning and microfluidic targeting of capture probes over optical nanostructures, we were able to immobilize four separate nucleic acid probes over individual photonic resonators, without cross-contamination between adjacent resonators. Immobilization of nucleic acid probes by silane and dendrimer linkages was confirmed by SEM and fluorescence microscopy. Using this improved patterning technique along with the demonstrated nucleic acid probe immobilization chemistry will aid in improving the sensitivity of label-free biosensors by eliminating surface contaminants that often remain after lithographic processing. Coupling microfluidic functionalization with parylene biopatterning further allows for multiplexed biopatterning without the deposition of PDMS residues onto the sensing surface. Although we have demonstrated this technique in an optical nanosensor application, it is well suited to a range of nanobiotechnology applications in which surface uniformity and cleanliness are necessary, including surface immobilized co-cultured cells, enzymes, antibodies, and neural growth factors.

## Acknowledgements

Support for this work was provided by the National Institutes of Health - National Institute of Biomedical Imaging and Bioengineering (NIH-NIBIB) under grant number R21EB007031 and the Defense Advanced Research Projects Agency Microsystems Technology Office (DARPA-MTO) Young Faculty Award Program. Portions of this work were performed at the Cornell Nanoscale Facility, a member of the National Nanotechnology Infrastructure Network, which is supported by the National Science Foundation (Grant ECS-0335765). This work made use of STC shared experimental facilities supported by the National Science Foundation under Agreement No. ECS-9876771. The authors gratefully acknowledge Rob Ilic for thoughtful discussions on parylene processing.

## References

- [1] M.A. Cooper, *Anal. Bioanal. Chem.* 377 (2003) 834.
- [2] D. Erickson, S. Mandal, A.H.J. Yang, B. Cordovez, *Microfluid. Nanofluid.* 4 (2008) 33.
- [3] J.N. Anker, W.P. Hall, O. Lyandres, N.C. Shah, J. Zhao, R.P. Van Duyne, *Nature Mater.* 7 (2008) 442.
- [4] F. Vollmer, S. Arnold, *Nat. Methods* 5 (2008) 591.
- [5] S. Mandal, D. Erickson, *Opt. Exp.* 16 (2008) 1623.
- [6] J.S. Daniels, N. Pourmand, *Electroanalysis* 19 (2007) 1239.
- [7] K. Lange, B.E. Rapp, M. Rapp, *Anal. Bioanal. Chem.* 391 (2008) 1509.
- [8] I. Barbulovic-Nad, M. Lucente, Y. Sun, M.J. Zhang, A.R. Wheeler, M. Bussmann, *Crit. Rev. Biotechnol.* 26 (2006) 237.
- [9] L.P. Xu, L. Robert, O.Y. Qi, F. Taddei, Y. Chen, A.B. Lindner, D. Baigl, *Nano Lett.* 7 (2007) 2068.
- [10] M. Mannini, D. Bonacchi, L. Zoppi, F.M. Piras, E.A. Speets, A. Caneschi, A. Cornia, A. Magnani, B.J. Ravoo, D.N. Reinhoudt, R. Sessoli, D. Gatteschi, *Nano Lett.* 5 (2005) 1435.
- [11] B. Ilic, H.G. Craighead, *Biomed. Microdevices* 2 (2000) 317.
- [12] J. Moran-Mirabal, C. Tan, R. Orth, E. Williams, H. Craighead, D. Lin, *Anal. Chem.* 79 (2007) 1109.
- [13] R.N. Orth, J. Kameoka, W.R. Zipfel, B. Ilic, W.W. Webb, T.G. Clark, H.G. Craighead, *Biophys. J.* 85 (2003) 3066.
- [14] K. Atsuta, H. Suzuki, S. Takeuchi, *J. Micromech. Microeng.* 17 (2007) 496.
- [15] N. Majid, S. Dabral, J.F. McDonald, *J. Electron. Mater.* 18 (1989) 301.
- [16] K.M. Byun, S.J. Yoon, D. Kim, S.J. Kim, *J. Opt. Soc. Am. A* 24 (2007) 522.
- [17] J.B. Fortin, T.M. Lu, *Thin Solid Films* 397 (2001) 223.
- [18] K.G. Pruden, K. Sinclair, S. Beaudoin, *J. Polym. Sci. Part A: Polym. Chem.* 41 (2003) 1486.
- [19] S. Mandal, J.M. Goddard, D. Erickson, *Lab Chip* (2009), doi:10.1039/b907826f.
- [20] N.V. Zaytseva, V.N. Goral, R.A. Montagna, A.J. Baeumner, *Lab Chip* 5 (2005) 805.
- [21] N.V. Zaytseva, R.A. Montagna, E.M. Lee, A.J. Baeumner, *Anal. Bioanal. Chem.* 380 (2004) 46.
- [22] S. Altschul, T. Madden, A. Schäffer, J. Zhang, Z. Zhang, W. Miller, D. Lipman, *Nucleic Acids Res.* 25 (1997) 3389.
- [23] E. Ghedin, N. Sengamalay, M. Shumway, J. Zaborsky, T. Feldblyum, V. Subbu, D. Spiro, J. Sitz, H. Koo, P. Bolotov, D. Dernovoy, T. Tatusova, Y. Bao, K. St George, J. Taylor, D. Lipman, C. Fraser, J. Taubenberger, S. Salzberg, *Nature* 437 (2005) 1162.

- [24] S.J.L. Wu, E.M. Lee, R. Putvatana, R.N. Shurtliff, K.R. Porter, W. Suharyono, D.M. Watts, C.C. King, G.S. Murphy, C.G. Hayes, J.W. Romano, *J. Clin. Microbiol.* 39 (2001) 2794.
- [25] J.M. Goddard, D. Erickson, *Anal. Bioanal. Chem.* 394 (2009) 469.
- [26] G.T. Hermanson, *Bioconjugate Techniques*, Academic Press, New York, 1996.
- [27] D.C. Duffy, J.C. McDonald, O.J.A. Schueller, G.M. Whitesides, *Anal. Chem.* 70 (1998) 4974.
- [28] M. Lee, P.M. Fauchet, *Opt. Exp.* 15 (2007) 4530.
- [29] L. Henke, N. Nagy, U.J. Krull, *Biosens. Bioelectron.* 17 (2002) 547.